2020 17th International Conference on Ubiquitous Robots (UR)
June 22-26, 2020. Kyoto, Japan

Persistent Area Coverage for Swarms Utilizing Deployment Entropy with Potential Fields

John D. Kelly[1], Daniel M. Lofaro[2], and Donald Sofge[2]

Abstract— **Our work focuses on persistent area coverage using a large number of agents. This is a valuable capability for multi-agent and swarm-based systems. Specifically, we strive to effectively disperse the agents throughout an area of interest such that it is sufficiently and persistently covered by the sensing sweeps of the agents. This capability can be applied toward tasks such as surveillance, target tracking, search and rescue, and exploration of unknown areas. Many methods can be implemented as behaviors for the agents to accomplish this. One strategy involves measuring area coverage using a measure known as deployment entropy, which relies on the area being divided into regions. Deployment entropy expresses the coverage of the area as the uniformity of agents per region across all regions. This strategy is useful due to its low computational complexity, scalability, and potential implementation on decentralized systems. Though previous results are promising, they focus on instantaneous area coverage and are not persistent. It is proposed in this paper that combining the split region strategy with the implementation of potential fields can retain the benefits of the split region strategy while increasing the spread of agents and therefore the total area that is persistently covered by the agents' sensors. This approach is implemented and demonstrated to be effective through simulations of various numbers and densities of agents. Ultimately, these studies showed that a greater spread of agents and increased sensor coverage is obtained when compared to previous results not using potential fields with deployment entropy.**

I. INTRODUCTION

Unmanned autonomous vehicles, especially those that can operate for long periods of time, have significant potential for surveillance tasks. Tasks such as persistent monitoring of an area, target tracking, search and rescue, and even planetary exploration could be advanced through the use of swarms of these vehicles. To effectively accomplish surveillance of an area of interest using a group of vehicles, it is vital that available vehicles are spread across the region such that it is covered by their sensing ranges. Thus, it is of value to produce strategies and methodologies for autonomous agents to effectively deploy across an area. Our work focuses on the latter, persistent area coverage using a large number of agents.

Because area coverage is a common aspect of tasks for which robotic swarms are needed, there is significant ongoing research into methods for a swarm of autonomous agents to sufficiently disperse throughout an area. Some recent strategies that show promise are those that are biologically inspired, as these lend themselves to be implemented as behaviors on decentralized swarm systems [1] [2]. Yang et al. created a dynamic algorithm that builds upon advances in biologically inspired algorithms based on the foraging patterns of bacteria using a Voronoi diagram-based strategy of dividing up the area of interest [3]. Other recent strategies include those that implement a leader-follower structure within the movement of the multi-agent system [4] [5] [6]. Due to its importance in many multi-agent and swarm-based tasks, numerous strategies and advances upon those strategies will certainly continue to emerge in the field.

In this paper a method for improving upon an existing strategy for persistent area coverage using a swarm of autonomous agents is explored. The existing strategy by Zheng-Jie et al. [7] provides a good foundation for further development due to the simplicity of the calculations required, which extend to the potential for scalability and ease of implementation as simple behaviors on autonomous systems.

II. BACKGROUND

Our work focuses on persistent area coverage (coverage over a length of time as opposed to one time point) using a large number of agents. The survey by Galceran et al. [8] focuses on instantaneous coverage path planning for individual or small teams of agents. This is a key difference between our work and typical coverage path planning goals and methods. Yang et al. [9] and Liu et al. [10] also focus on instantaneous area coverage instead of persistent area coverage and are thus not as applicable to our problem. Gazi et al. [11] does match our problem more closely, however they assume that each agent "knows the exact position of all the other individuals." We are specifically only looking at the more realistic case of an agent only knowing state information about its nearest neighbors. To the best of our knowledge the literature has not adequately addressed the challenge of using a multitude of agents for persistent area coverage with using only state information from the local agents. This is what makes our work unique.

Additionally, in their paper [12] Li and Zhang established a novel quantitative method, known as deployment entropy, to evaluate the quality of coverage of sensors in an area. Deployment entropy is a measure which "expresses the uniformity of the deployment of sensors" among a number of regions in an area. Sensing coverage has historically been measured as the ratio of the area that can be sensed over the

[1]Kelly, J. is a Researcher with the RISE Laboratory at Naval Air Warfare Center - Aircraft Division, Lakehurst, NJ, USA john.d.kelly@navy.mil

[2]Lofaro, D. and Sofge, D. are Researcher with the Distributed Autonomous Systems Group at the U.S. Naval Research Laboratory, 4555 Overlook Ave SW, Washington DC, 20375, USA daniel.lofaro@nrl.navy.mil and donald.sofge@nrl.navy.mil

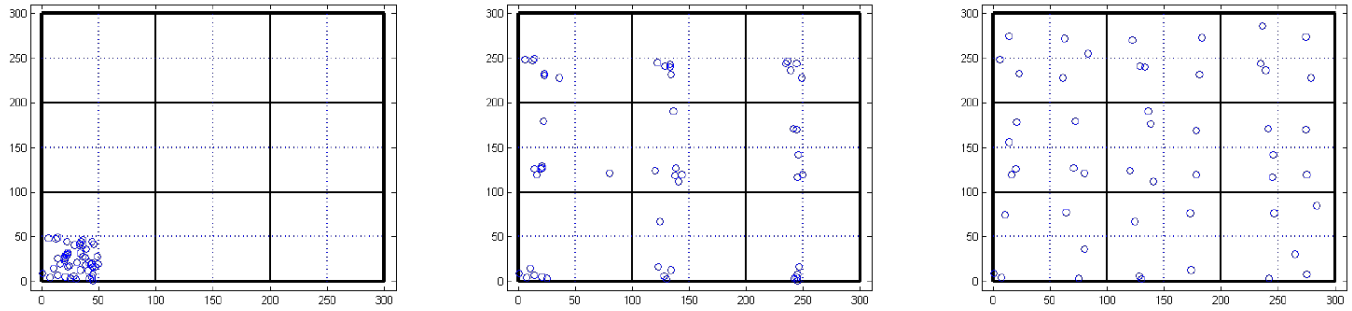

(a) Initial Stage (b) After Global Level Redeployment (c) After Local Level Redeployment

Fig. 1. (left to right) Example two-level redeployment [7]

entire area of interest. Deployment entropy was proposed as a measure to accomplish effective sensor deployment and coverage that is less calculation-intensive. Using deployment entropy requires dividing the area of interest into a number of smaller regions, and is based on how balanced the amount of sensors per region is across all of the regions in the area of interest. In their paper [7] Zheng-jie and Wei adapt deployment entropy as a method for distribution of micro aerial vehicles (MAVs) for the purpose of surveillance of an area. Deployment entropy is described by Equation 1:

$$H = -\sum_{i=1}^{n} p_i \ln p_i \tag{1}$$

where

$$p_i = \frac{ratio_i}{\sum_{k=1}^{n} ratio_k} \tag{2}$$

$$ratio_i = \frac{N_i}{S_i} \tag{3}$$

$$N_{total} = \sum_{i=1}^{n} N_i \tag{4}$$

$$S_{total} = \sum_{i=1}^{n} S_i \tag{5}$$

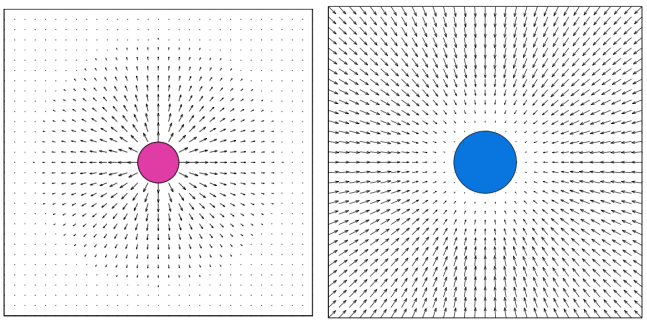

Fig. 2. (LEFT) Model of repulsive potential field. (RIGHT) Model of attractive potential field [13]

Though the researchers present a scenario utilizing a swarm of MAVs, this strategy can be utilized for any group of autonomous agents. For the use case of deployment of a swarm of autonomous agents, n is the number of regions that the area has been divided into, N_i is the number of agents in the ith region, S_i is the area of the ith region, $ratio_i$ is the ratio of the amount of agents in the ith region to the area of the ith region, and S_{total} is the total area of the overall area of interest. The value of deployment entropy for a given case reaches its maximum when the value of the ratio for each region is equal to N_{total}/S_{total}. Thus, maximizing the deployment entropy will maximize the uniformity of the distribution of agents among the regions.

Zheng-jie and Wei [7] propose a two-level redeployment method and establish a number of rules for implementation using MAVs toward the goal of achieving maximum deployment entropy. The scenario for implementation is that a number of MAVs have been deployed into the area of interest, either into one region of the area or randomly dispersed throughout the area. To create the regions for the implementation of deployment entropy, the area is partitioned into a grid of relatively large cells. The regions are then iterated through as agents are redeployed one at time to neighboring regions where the ratio of agents to area is lower. Their proposed strategy is to deploy the agents into the area and then begin redeploying them one at a time. After the redeployment of a MAV, the deployment entropy is recalculated. This iteration repeats until a desired deployment entropy is reached. The regions are then divided into a number of sub-regions, and the redeployment is repeated on a local level within the larger regions. This is done to increase the sensor coverage of the area of interest. They provide pseudocode for their implementation in their paper, shown in Algorithm 1.

This implementation is based on a number of rules to govern the movements of the MAVs during redeployment. The first is the previously mentioned grid-based partitioning method for the division of the area into regions, which simplifies planning and area computation. The second rule is that every region or sub-region can only interact with its neighboring regions or sub-regions. The third is that MAVs can only relocate themselves from one region or sub-region to one with a lower ratio. The fourth is that for a MAV to move between two regions or sub-regions, the difference between their numbers of MAVs must be greater than one, which ensures the deployment reaches a final stable state.

The final rule is that only one MAV can be selected to move for each region on each iteration, and the MAV that moves is the one which is the shortest direct distance away from the center of the region which is being moved into. See Figure 1 for an example two-level redeployment scenario. In this example, the thick black lines represent the divisions for the larger regions, the dotted blue lines represent the divisions for the sub-regions, and the blue circles represent the agents.

The characteristics of deployment entropy as a strategy for a surveillance application and the rules that Zheng-jie and Wei introduce for their implementation make it useful for applications where autonomous agents need to distribute themselves across an area while using decentralized control. The rule which provides the constraint that regions and sub-regions only interact with their neighbors means that only short-range communication is required. Agents only need to communicate with those in their own region and those in adjacent ones to coordinate moves. Agents only need to know their own location, and do not need to know the overall global state of all agents. Decentralized control is desirable to provide greater security compared to centralized control for multi-agent systems due to greater fault tolerance, as discussed by Jiménez et al. [14]. The system can continue to function even if one agent fails.

III. METHODOLOGY

This section discusses how the deployment entropy strategy of agent distribution was implemented in simulation and how potential fields were implemented to increase the spread of agents. A script was created that can generate a simulated deployment given user-input quantities. The user can input the number of agents in the scenario, the dimensions of the area under study, the numbers of rows and columns of regions, and in which region the agents enter the area of interest at the beginning of the simulation. Following the method laid out in the pseudocode in Figure 1, the user sets goal deployment entropy values for the global and local redeployment phases and the simulation iterates through all regions redeploying agents to neighboring regions and sub-regions until these goal values are reached. When an agent moves from one region to another, it chooses a random location within that region.

The simulation results obtained using the deployment entropy method with a two-level redeployment scheme were promising, considering their previously noted potential for use with decentralized control and scalability due to the simple calculations required. However, one undesirable trend with the method described emerged as simulations were run. Due to the fact that that the agents that moved to neighboring regions were the ones closest to the centers of those neighboring regions, the agents that remained behind were often clustered in a corner far from their neighbors, especially in cases where there were large numbers of agents. The implementation of potential fields [13] was considered as a possible solution to this issue.

We initially considered implementation of a repulsive field between agents after the two-level redeployment would produce a significant improvement in the spread of the agents. A repulsive potential field can be modeled as shown in Figure 2. In that diagram, the magenta circle represents the object generating the repulsive field, and the magnitude of the repulsive force is proportional to the distance from the object. Outside of the field's range (shown in the space where the black arrows become black dots), the magnitude of the repulsive force is zero. The mathematics for implementation of a repulsive potential field can be seen below:

Algorithm 1: Pseudocode for implementation of deployment entropy area coverage methodology [7]

```
1  Partition the interested field into n grids, N MAVs
     are deployed in the interested field;
2  for i=1 to n do
3      compute the MAVs number in each grid, N_i;
4      compute the ratio of each grid;
5  end
6  Compute the theoretical deployment entropy;
7  Compute the current deployment entropy;
8  while the current deployment entropy is less than the
     theoretical deployment entropy do
9      for i=1 to n do
10         if the ratio difference between i^th grid and its
             neighbour grids exceed the ratio difference
             threshold then
11             for j=1 to N_i do
12                 compute the distance between MAVs
                     in the i^th grid and each neighbour
                     grid centre;
13             end
14             Find the shortest distance and record the
                 MAV ID=j;
15             Move the j^th MAV to the neighbour grid;
16         end
17         Re-compute number of MAVs in each grid,
             N_i;
18         Re-compute deployment entropy after node
             movements;
19     end
20 end
21 Partition each sub-grid into m sub-grids;
22 for i = 1 to n do
23     for j = 1 to m do
24         Repeat compute process steps 9-19 for each
             sub-grid
25     end
26 end
```

$$x = \begin{cases} -sign(cos\theta) \cdot \infty & : \quad d < r \\ -\beta(s + r - d)cos(\theta) & : \quad r \leq d \leq s + r \\ 0 & : \quad d > s + r \end{cases} \tag{6}$$

$$y = \begin{cases} -sign(sin\theta) \cdot \infty & : \quad d < r \\ -\beta(s + r - d)sin(\theta) & : \quad r \leq d \leq s + r \\ 0 & : \quad d > s + r \end{cases} \tag{7}$$

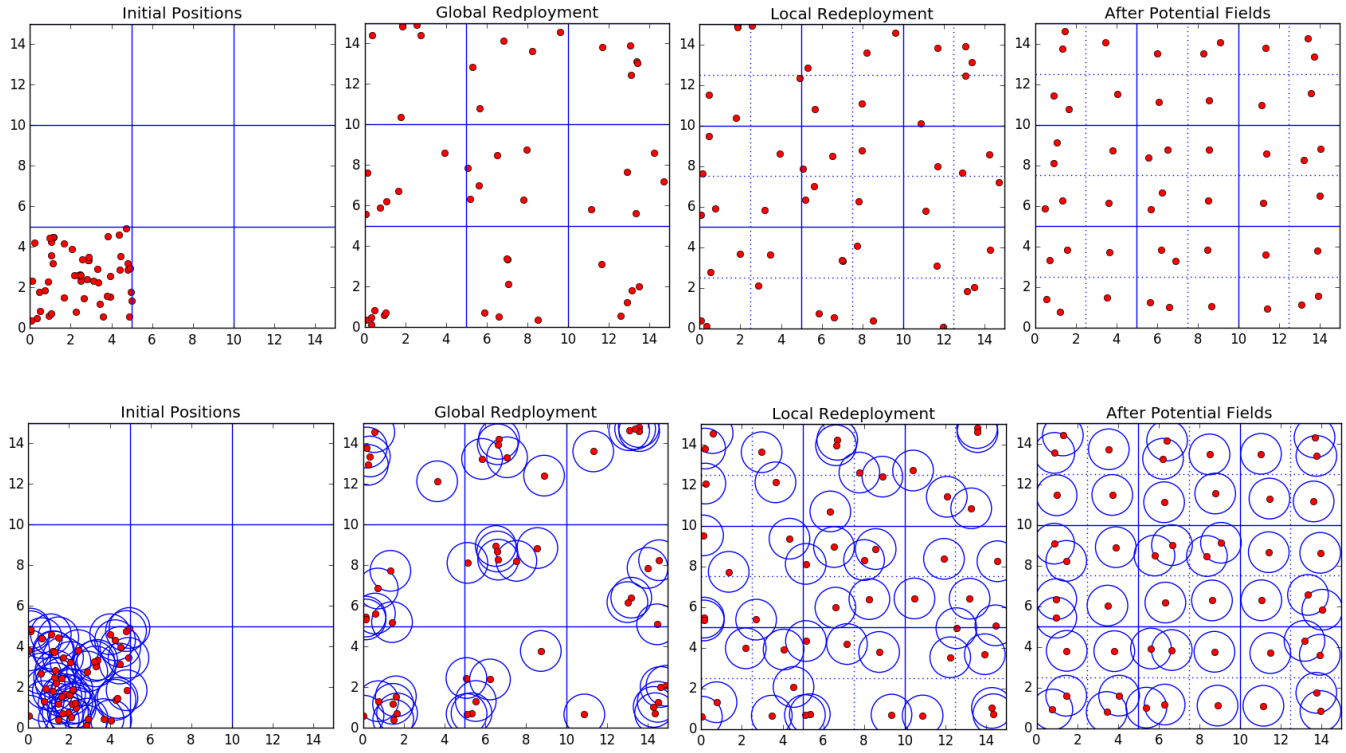

Fig. 3. (**TOP** - left to right) Results of simulated 50 agent redeployment. (**BOTTOM** - left to right) Results of simulated 50 agent redeployment with visualized sensor coverage areas.

In these equations, d is the distance between the agent and the center of the obstacle generating the field, r is the radius of the obstacle, s is the radius of the potential field, Θ is the angle between the agent and the obstacle found using the *atan2* function, and β is the field strength.

However, because the agents were often grouped in the corners of regions following the local redeployment stage, the agents repelling each other often just pushed them into the boundaries of their sub-region without significantly increasing their spread. To produce a better spread, and therefore increased sensor coverage, over the sub-region, the agents would have to be repelled from somewhere closer to the center of the sub-region. From this came the idea of first having an attractive force to move agents toward the center, followed by a repulsive force away from each other. An attractive potential field can be modeled as shown in Figure 2. In that diagram, the blue circle represents the object generating the attractive field, and the magnitude of the attractive force is inversely proportional to the distance from the object. The mathematics for implementation of an attractive potential field can be seen below:

$$x = \begin{cases} 0 & : \quad d < r \\ \alpha(d-r)cos(\theta) & : \quad r \leq d \leq s+r \\ \alpha s(cos(\theta)) & : \quad d > s+r \end{cases} \tag{8}$$

$$y = \begin{cases} 0 & : \quad d < r \\ \alpha(d-r)sin(\theta) & : \quad r \leq d \leq s+r \\ \alpha s(sin(\theta)) & : \quad d > s+r \end{cases} \tag{9}$$

In these equations, d is the distance between the agent and the center of the obstacle generating the field, r is the radius of the obstacle, s is the radius of the potential field, Θ is the angle between the agent and the obstacle found using the *atan2* function, and α is the field strength.

The potential field math was implemented within the redeployment simulation to begin after the desired deployment entropy value is reached following the local redeployment. In the current form of the simulation, the math presented above (Eqns. (6)-(9)) is used to compute a position change in the agents, first toward the center of their sub-regions assuming that the attractive field was being generated by a point at the center of the sub-region, and then away from each other. If the potential field forces would push an agent outside of its sub-region, it simply stops at the boundary. The field strengths were manually tuned based on the size of the area in simulation (which was based on a testing area in the real world).

IV. RESULTS

A 50-agent deployment was simulated utilizing the deployment entropy strategy with two-level redeployment and potential fields, the results of which can be seen in Figure 3.

The red dots are the agents in the scenario, the blue solid lines designate the larger regions, and the dotted blue lines

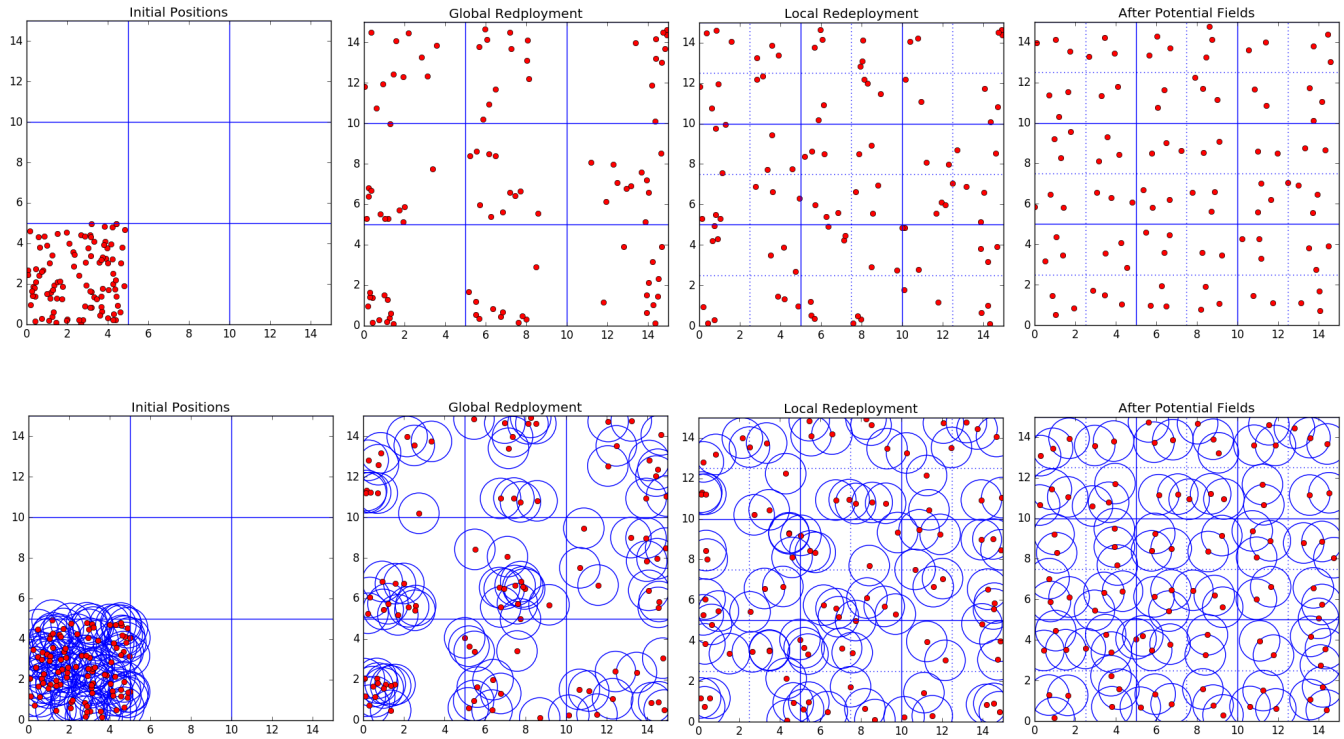

Fig. 4. (**TOP** - left to right) Results of simulated 100 agent redeployment. (**BOTTOM** - left to right) Results of simulated 100 agent redeployment with visualized sensor coverage areas.

designate the sub-regions. After the global redeployment into the divided regions and the local redeployment into the sub-regions, it can be seen that some of the agents' final positions are clustered together, often in corners. After the application of the attractive field toward the center followed by the repulsive fields between agents, it can be seen that there is a much more even spread of agents. If you envision the agents as airborne autonomous systems surveying the ground, the area that the sensor can view on the ground could be a circular area. Figure 3 is a representation of what this 50-agent redeployment scenario looks like with the sensor coverage areas of the agents represented by blue circles around them. In this figure, it can be seen that after the local redeployment there is still overlap between agents' sensor areas, while after the potential field application there is less overlap and greater sensor coverage of the area of interest overall.

In situations with large numbers of agents compared to the number of total sub-regions, the clustering-into-corners effect during redeployment can be even more significant. See Figures 4 for another simulation with 100 agents with the same area and region divisions as the 50-agent simulation. It can be seen that the application of potential fields yields a greater agent spread within sub-regions and greater sensor coverage.

A. *Comparison*

Now we compare our method of using the potential fields to that of using the traditional redeployment method (i.e. without potential fields). To do this we look at the mean distance of the closest six agents to each agent. The closest six agents metric is chosen because that is the number of agents surrounding each agent if they formed a two dimensional (2D) crystalline structure where all agents are of equal distance from one another. An example of this can be seen in Figure 5. Please note that all adjacent agents are the same distance from each other. The angle formed between any three adjacent agents is 60^o. This deployment is the optimal deployment for even area coverage.

We define the theoretical minimum but equal distance between all agents as L_{min}. For ease of calculation we assume that we have a square field (operating space) and that you can not have a fraction of an agent.

$$L_{min} = \frac{L}{\lceil N^{\frac{1}{2}} - 1 \rceil} \tag{10}$$

where L is the length of one side of the square field and N is the number of agents on one side of the crystalline box. The -1 is added because we assume that there can be an agent at the edges of the square field. N is defined as:

$$N = \left(\frac{M}{2}\right)^{\frac{1}{2}} \tag{11}$$

where M is the number of agents.

For the first group of simulations, whose data is represented in Figure 6 and Tables I, II, III, IV, and V, a repulsive potential field strength (β) of 0.5 is used in equations (6) and (7). The mean of the distances between agents is roughly equivalent before and after using potential fields.

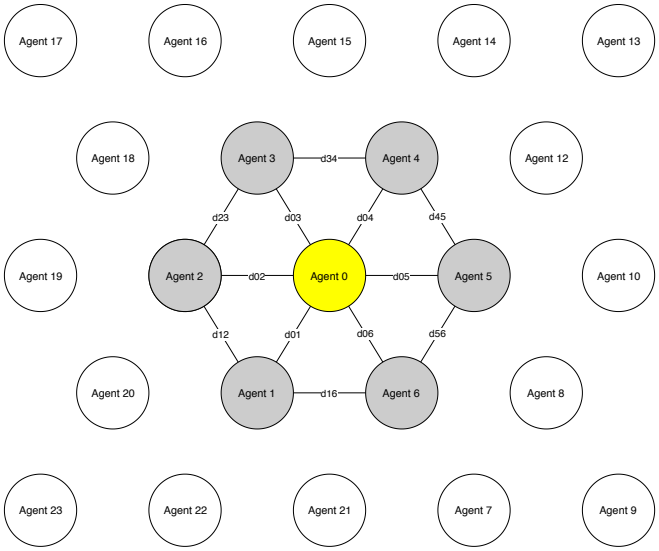

Fig. 5. Example of the optimal (most uniform) crystalline structure. All adjacent agents are equal distance from one another. The angle formed between any three adjacent agents is 60^o. In this case Agent 0 is the agent of interest. Note that $d01 = d02 = d03 = \cdots = d56$.

The standard deviation is lower after field implementation for lower numbers of agents, but increases at 500 and 1000 agents. The latter increase at 500 in Figure 6 will be referred to ask "the knee" from this point forward. The presence of the knee indicates that the agent spread is less uniform at this field strength for higher numbers of agents. This effect is due to the increasing density of the repulsive field strength creating more "energy" in the system. If we decrease the β energy from the potential fields, to decrease the density, we will see the knee move to the right. For the second group of simulations, whose data is represented in Figure 7 and Tables VI, VII, VIII, IX, and X, a repulsive potential field strength (β) of 0.1 is used. The knee is not not present up to 1000 agents. The standard deviation of mean distances after potential field implementation remains lower than before for all five agent quantities simulated. These results indicate that in order to obtain the most uniform spread, repulsive field strength must be tuned with respect to the number of agents being deployed.

B. Discussion

It is noted that the mean of the distances between adjacent agents is similar to both the potential fields method and the non-potential fields method. The standard deviation of the mean distance between adjacent agents remains considerably lower for the potential fields method. This means that we can use a more uniformly distributed set of agents using the potential fields method vs. traditional methods. We expect that with the increase of the number of agents that the standard deviation of the mean distance will decrease due to the decreasing mean distance. An interesting effect of the potential fields method can be seen in the plot of the standard deviation of the mean distance between agents in Figure 7. This plot shows that you will need approximately

TABLE I

STATISTICS FOR REDEPLOYMENT OF 50 AGENTS BEFORE AND AFTER IMPLEMENTATION OF POTENTIAL FIELDS. NOTE: REPULSIVE FIELD STRENGTH FOR THIS SIMULATION IS 0.5.

50 Agents	*Before Fields*	*After Fields*
Mean of Mean Distances	2.685	2.669
Std. Dev. of Mean Distances	0.531	0.321
Std. Dev. of All Std. Dev.	0.432	0.305
Mean of All Std. Dev.	0.942	0.708

TABLE II

STATISTICS FOR REDEPLOYMENT OF 100 AGENTS BEFORE AND AFTER IMPLEMENTATION OF POTENTIAL FIELDS. NOTE: REPULSIVE FIELD STRENGTH FOR THIS SIMULATION IS 0.5.

100 Agents	*Before Fields*	*After Fields*
Mean of Mean Distances	1.752	1.752
Std. Dev. of Mean Distances	0.381	0.236
Std. Dev. of All Std. Dev.	0.269	0.140
Mean of All Std. Dev.	0.646	0.536

180 agents using the non-potential fields method to get the same standard deviation of mean distances between agents as you get with 50 agents using the potential fields method. This shows that the potential fields method out-performs the non-potential fields method in creating a uniformly distributed set of agents.

V. CONCLUSION

In this paper the problem of agent congestion when utilizing the deployment entropy-based solution for area coverage surveillance using a swarm of autonomous agents was considered. The concept of deployment entropy originated as a method for coverage analysis of wireless sensor networks and was later proposed as a method for area coverage of a swarm of micro aerial vehicles. Deployment entropy is useful for its scalability and potential for implementation on systems of agents using decentralized control. The implementation of a simulation of the deployment entropy swarm area coverage

TABLE III

STATISTICS FOR REDEPLOYMENT OF 200 AGENTS BEFORE AND AFTER IMPLEMENTATION OF POTENTIAL FIELD. NOTE: REPULSIVE FIELD STRENGTH FOR THIS SIMULATION IS 0.5.

200 Agents	*Before Fields*	*After Fields*
Mean of Mean Distances	1.053	1.199
Std. Dev. of Mean Distances	0.278	0.180
Std. Dev. of All Std. Dev.	0.156	0.106
Mean of All Std. Dev.	0.397	0.329

TABLE IV

STATISTICS FOR REDEPLOYMENT OF 500 AGENTS BEFORE AND AFTER IMPLEMENTATION OF POTENTIAL FIELDS. NOTE: REPULSIVE FIELD STRENGTH FOR THIS SIMULATION IS 0.5.

500 Agents	*Before Fields*	*After Fields*
Mean of Mean Distances	0.546	0.569
Std. Dev. of Mean Distances	0.236	0.366
Std. Dev. of All Std. Dev.	0.087	0.148
Mean of All Std. Dev.	0.182	0.208

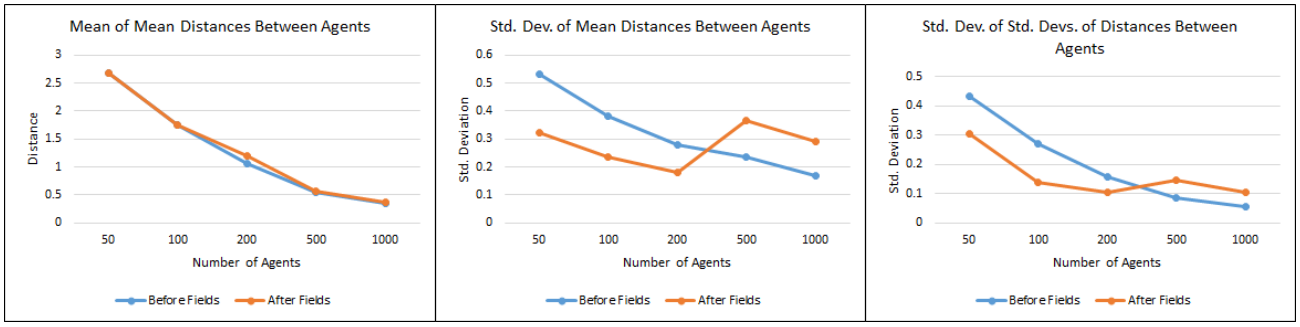

Fig. 6. Statistical plots of (RIGHT) the mean distance between neighboring agents. (MIDDLE) the standard deviation of the mean of the distance between neighboring agents. (RIGHT) the standard deviation of the standard deviation mean standard deviation between neighboring agents. Note: These were taken for the potential fields case and the non-potential fields case for the closest six agents. The repulsive field strength (β) for all simulations is 0.5.

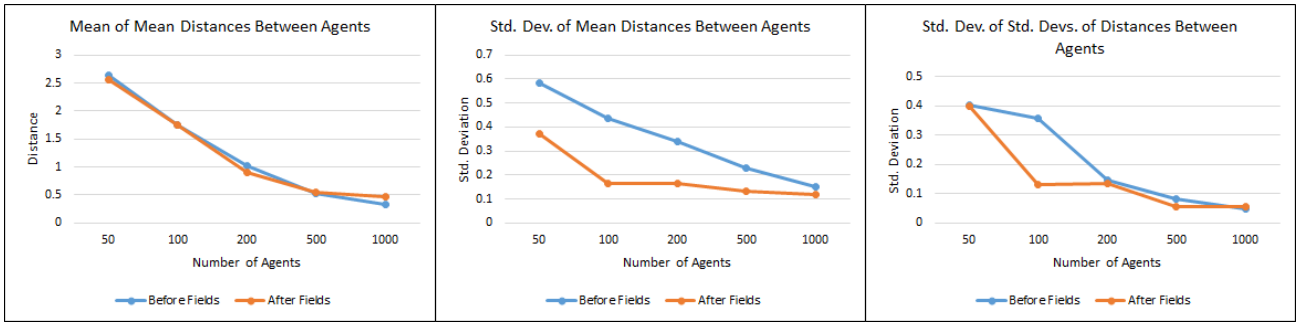

Fig. 7. Statistical plots of (RIGHT) the mean distance between neighboring agents. (MIDDLE) the standard deviation of the mean of the distance between neighboring agents. (RIGHT) the standard deviation of the standard deviation mean standard deviation between neighboring agents. Note: These were taken for the potential fields case and the non-potential fields case for the closest six agents. These plots differ from those in Figure 6 as field strength as decreased for the simulations with larger numbers of agents. The repulsive field strength (β) for all simulations is 0.1.

TABLE V

STATISTICS FOR REDEPLOYMENT OF 1000 AGENTS BEFORE AND AFTER IMPLEMENTATION OF POTENTIAL FIELDS. NOTE: REPULSIVE FIELD STRENGTH FOR THIS SIMULATION IS 0.5.

1000 Agents	*Before Fields*	*After Fields*
Mean of Mean Distances	0.345	0.378
Std. Dev. of Mean Distances	0.167	0.292
Std. Dev. of All Std. Dev.	0.055	0.105
Mean of All Std. Dev.	0.109	0.120

TABLE VI

STATISTICS FOR REDEPLOYMENT OF 50 AGENTS BEFORE AND AFTER IMPLEMENTATION OF POTENTIAL FIELDS. NOTE: REPULSIVE FIELD STRENGTH FOR THIS SIMULATION IS 0.1.

50 Agents	*Before Fields*	*After Fields*
Mean of Mean Distances	2.644	2.563
Std. Dev. of Mean Distances	0.582	0.373
Std. Dev. of All Std. Dev.	0.404	0.398
Mean of All Std. Dev.	0.904	0.741

TABLE VII

STATISTICS FOR REDEPLOYMENT OF 100 AGENTS BEFORE AND AFTER IMPLEMENTATION OF POTENTIAL FIELDS. NOTE: REPULSIVE FIELD STRENGTH FOR THIS SIMULATION IS 0.1.

100 Agents	*Before Fields*	*After Fields*
Mean of Mean Distances	1.748	1.745
Std. Dev. of Mean Distances	0.434	0.166
Std. Dev. of All Std. Dev.	0.356	0.132
Mean of All Std. Dev.	0.664	0.839

TABLE VIII

STATISTICS FOR REDEPLOYMENT OF 200 AGENTS BEFORE AND AFTER IMPLEMENTATION OF POTENTIAL FIELDS. NOTE: REPULSIVE FIELD STRENGTH FOR THIS SIMULATION IS 0.1.

200 Agents	*Before Fields*	*After Fields*
Mean of Mean Distances	1.021	0.901
Std. Dev. of Mean Distances	0.339	0.166
Std. Dev. of All Std. Dev.	0.148	0.136
Mean of All Std. Dev.	0.389	0.551

TABLE IX

STATISTICS FOR REDEPLOYMENT OF 500 AGENTS BEFORE AND AFTER IMPLEMENTATION OF POTENTIAL FIELDS. NOTE: REPULSIVE FIELD STRENGTH FOR THIS SIMULATION IS 0.1.

500 Agents	*Before Fields*	*After Fields*
Mean of Mean Distances	0.531	0.556
Std. Dev. of Mean Distances	0.231	0.133
Std. Dev. of All Std. Dev.	0.083	0.057
Mean of All Std. Dev.	0.174	0.165

TABLE X

STATISTICS FOR REDEPLOYMENT OF 1000 AGENTS BEFORE AND AFTER IMPLEMENTATION OF POTENTIAL FIELDS. NOTE: REPULSIVE FIELD STRENGTH FOR THIS SIMULATION IS 0.1.

1000 Agents	*Before Fields*	*After Fields*
Mean of Mean Distances	0.332	0.473
Std. Dev. of Mean Distances	0.151	0.121
Std. Dev. of All Std. Dev.	0.050	0.054
Mean of All Std. Dev.	0.106	0.146

strategy was discussed, followed by the introduction of the problem of agent congestion following the two-level redeployment scheme proposed by Zheng-Jie and Wei [7]. Potential fields were proposed as a solution to this congestion. It was shown that the implementation of two potential field phases, an attraction toward the center of sub-regions followed by a repulsion between agents, can increase spread of agents within sub-regions and overall coverage of the area of interest. Statistical analysis concluded that implementation of potential fields increased mean distance between agents and lowered the standard deviation, indicating that there is a greater, more uniform spread, resulting in greater area coverage and more efficient usage of agent resources. Finally, it was shown that the potential fields method out-performs the non-potential fields method in creating a uniformly distributed set of agents.

VI. FUTURE WORK

In this work we focused on persistent area coverage using a large number of agents. In this vein we showed that a greater spread of agents and increased sensor coverage is obtained when compared to previous results not using potential fields with deployment entropy. Additionally, we found that there may be a point (number of agents) in which our method becomes less efficient than the baseline method. This is especially interesting and will require additional mathematical modeling to determine why we obtained this behavior.

There are a number of possible paths to follow to take this research forward. In the simulations presented in this paper, the field strengths of the potential fields were manually adjusted, but it would be desirable to create a methodology for automatically deciding these characteristics. This method could potentially factor in the number of agents, the size of the sub-regions, and/or the size of the sensing area of the agents. Such a method would be of particular interest if the agents have different sensing areas, either due to having different sensors or by completing a surveillance mission at different altitudes. As the statistical results showed that repulsive field strength has a relationship with the degree and uniformity of the spread of agents as the number of agents increases, a mathematical relationship could be developed in order to determine what potential field strength results in the optimal coverage. Additional research could be conducted into fully exploring the effect that varying field strength values have upon the area coverage. Incorporating a third dimension into the algorithm would introduce additional nuances and challenges to this method. A valuable challenge to pursue would be implementing the deployment entropy area coverage strategy in the real-world in a truly decentralized way. This can be done on our lighter-than-air aerial agents (LTA3) from our previous work [15]–[19]. This would involve implementing it as a behavior on autonomous mobile robots who only have access to their own location and local information from neighboring agents, and implementing a method of the agents knowing when redeployment efforts have ended and to begin potential field use to increase spread.

ACKNOWLEDGMENT

This work was performed at the U.S. Naval Research Laboratory and was funded by the Office of Naval Research under contract N0001418WX01828 for the project "Coherence and Decoherence of Patterns in Swarms with Potential Collisions". The views, positions and conclusions expressed herein reflect only the authors' opinions and expressly do not reflect those of the Office of Naval Research, nor those of the U.S. Naval Research Laboratory.

REFERENCES

[1] K. M. Passino, "Biomimicry of bacterial foraging for distributed optimization and control," *IEEE control systems magazine*, 2002.
[2] M. S. Couceiro, C. M. Figueiredo, R. P. Rocha, and N. M. Ferreira, "Darwinian swarm exploration under communication constraints: Initial deployment and fault-tolerance assessment," *Robotics and Autonomous Systems*, vol. 62, no. 4, pp. 528–544, 2014.
[3] B. Yang, Y. Ding, and K. Hao, "Area coverage searching for swarm robots using dynamic voronoi-based method," in *2015 34th Chinese Control Conference (CCC)*, pp. 6090–6094, IEEE, 2015.
[4] L. Xiao-Yuan, H. Na-Ni, and G. Xin-Ping, "Leader-following formation control of multi-agent networks based on distributed observers," *Chinese Physics B*, vol. 19, no. 10, p. 100202, 2010.
[5] A.-H. Hu, J.-D. Cao, M.-F. Hu, and L.-X. Guo, "Consensus of a leader-following multi-agent system with negative weights and noises," *IET Control Theory & Applications*, vol. 8, no. 2, pp. 114–119, 2014.
[6] J. Qin, C. Yu, and H. Gao, "Coordination for linear multiagent systems with dynamic interaction topology in the leader-following framework," *IEEE Transactions on Industrial Electronics*, 2013.
[7] W. Zheng-Jie and L. Wei, "A solution to cooperative area coverage surveillance for a swarm of mavs," *International journal of advanced robotic systems*, vol. 10, no. 12, p. 398, 2013.
[8] E. Galceran and M. Carreras, "A survey on coverage path planning for robotics," *Robotics and Autonomous Systems*, 2013.
[9] B. Yang, Y. Ding, and K. Hao, "Area coverage searching for swarm robots using dynamic voronoi-based method," in *2015 34th Chinese Control Conference (CCC)*, pp. 6090–6094, July 2015.
[10] X. Liu and Y. Tan, "Adaptive potential fields model for solving distributed area coverage problem in swarm robotics," in *Advances in Swarm Intelligence* (Y. Tan, H. Takagi, Y. Shi, and B. Niu, eds.), (Cham), pp. 149–157, Springer International Publishing, 2017.
[11] V. Gazi and K. M. Passino, "A class of attractions/repulsion functions for stable swarm aggregations," *International Journal of Control*, vol. 77, no. 18, pp. 1567–1579, 2004.
[12] W. Li and W. Zhang, "Coverage analysis and active scheme of wireless sensor networks," *IET wireless sensor systems*, 2012.
[13] M. A. Goodrich, "Potential fields tutorial," *Class Notes*, vol. 157, 2002.
[14] A. C. Jiménez, V. García-Díaz, and S. Bolaños, "A decentralized framework for multi-agent robotic systems," *Sensors*, vol. 18, no. 2, p. 417, 2018.
[15] T. Schuler, D. Lofaro, L. McGuire, A. Schroer, T. Lin, and D. Sofge, "A study of robotic swarms and emergent behaviors using 25+ real-world lighter-than-air autonomous agents (lta3)," in *2019 3rd International Symposium on Swarm Behavior and Bio-Inspired Robotics (SWARM)*, 2019.
[16] J. Gibson, T. Schuler, D. Sofge, and D. Lofaro, "Swarm and multi-agent time-based path planning for lta3 systems," in *World Scientific: Unmanned Systems*, 2020.
[17] D. Lofaro and D. Sofge, "Multimodal control of lighter-than-air agents," in *Proceedings of the 20th ACM International Conference on Multimodal Interaction*, ICMI 2018, ACM, 2018.
[18] D. Srivastava, D. Lofaro, T. Schuler, and D. Sofge, "Gesture-based interface for multi-agent and swarm formation control," in *2019 3rd International Symposium on Swarm Behavior and Bio-Inspired Robotics (SWARM)*, 2019.
[19] J. Gibson, T. Schuler, D. Sofge, and D. Lofaro, "Multi-agent time-based a* path planning on lighter-than-air autonomous agents," in *IEEE International Conference on Cybernetics and Intelligent Systems, and Robotics, Automation and Mechatronics (CIS-RAM)*, 2019.